Megacam: paving the focal plane of the MMT with silicon

B. A. McLeod, T. M. Gauron, J. C. Geary, M. P. Ordway, and J. B. Roll, Jr.

Harvard-Smithsonian Center for Astrophysics, 60 Garden St., Cambridge, MA 02138 USA

ABSTRACT

Megacam is a 36 CCD mosaic camera that will cover a $24' \times 24'$ field of view at the f/5 wide-field focus of the converted 6.5 m Multiple Mirror Telescope. The mosaic is a 9×4 array of thinned 2048×4608 pixel CCDs with 13.5μm pixels. The CCDs are dual-output EEV devices in a custom package to allow the devices to be closely butted on all four sides. The dewar will be mounted to a 2 m diameter assembly that contains the filter wheels (for 30×30 cm filters) and the shutter. Telescope guiding will be accomplished with two additional CCDs mounted at the edges of the focal plane. The guider CCDs will be operated slightly defocused, one on either side of focus, to allow simultaneous focusing and guiding. Guide stars will be selected by reading out the full guider frame, after which only a small area surrouding the guide star will be read out. Our simulations show that the defocused guide star images will also be useful for low order wavefront sensing, allowing corrections to the telescope collimation. We are developing a new CCD controller capable of reading the full Megacam in 24 seconds. This controller will also be used to operate the guide chips.

Keywords: CCDs, imaging, cameras, astronomy, telescope guiding

1. INTRODUCTION

The Multiple Mirror Telescope on Mt. Hopkins, Arizona, is currently being converted from six 1.8 m telescopes to a single 6.5 m diameter mirror. The imaging configuration of the f/5 wide-field corrected Cassegrain focus will provide a $35'$ diameter field, which is flat and has $0\farcs1$ RMS image quality from 0.35 to 1.0μm. Megacam will populate this focal plane with state-of-the-art CCD detectors. The mosaic will consist of 18432×18432 $0\farcs08$ pixels. We have previously described a conceptual design for this camera.[1] In this paper we provide a more detailed description of the planned hardware.

2. CAMERA HOUSING

The camera housing, or "topbox", is a 2 m diameter, 0.3 m deep steel structure that contains the shutter and filter wheels, and provides a rigid interface between the CCD Dewar and the telescope. A cut-away view of the assembly is shown in Figure 1.

2.1. Filter Wheels

The housing contains two overlapping filter wheels, each with five slots. Normally one of these slots will be left blank in each filter wheel, allowing a choice of eight filters at any given time. The filter wheels are driven from their centers with a DC-servo motor, harmonic drive gear reduction, and a rotary encoder, which provides a lateral repeatability of 10μm at the radius of the filters. This high repeatability allows us the option to use segmented filters without incurring flat-fielding errors due to misregistration of the filters. Each filter wheel is composed of two steel facesheets separated by a web of reinforcements. Filters are mounted in a steel frame that is inserted between the two facesheets of the filter wheel from access ports on each side of the housing.

Other author information: (Send correspondence to B.A.M.)
Email: bmcleod,jgeary,tgauron,mordway,jroll@cfa.harvard.edu

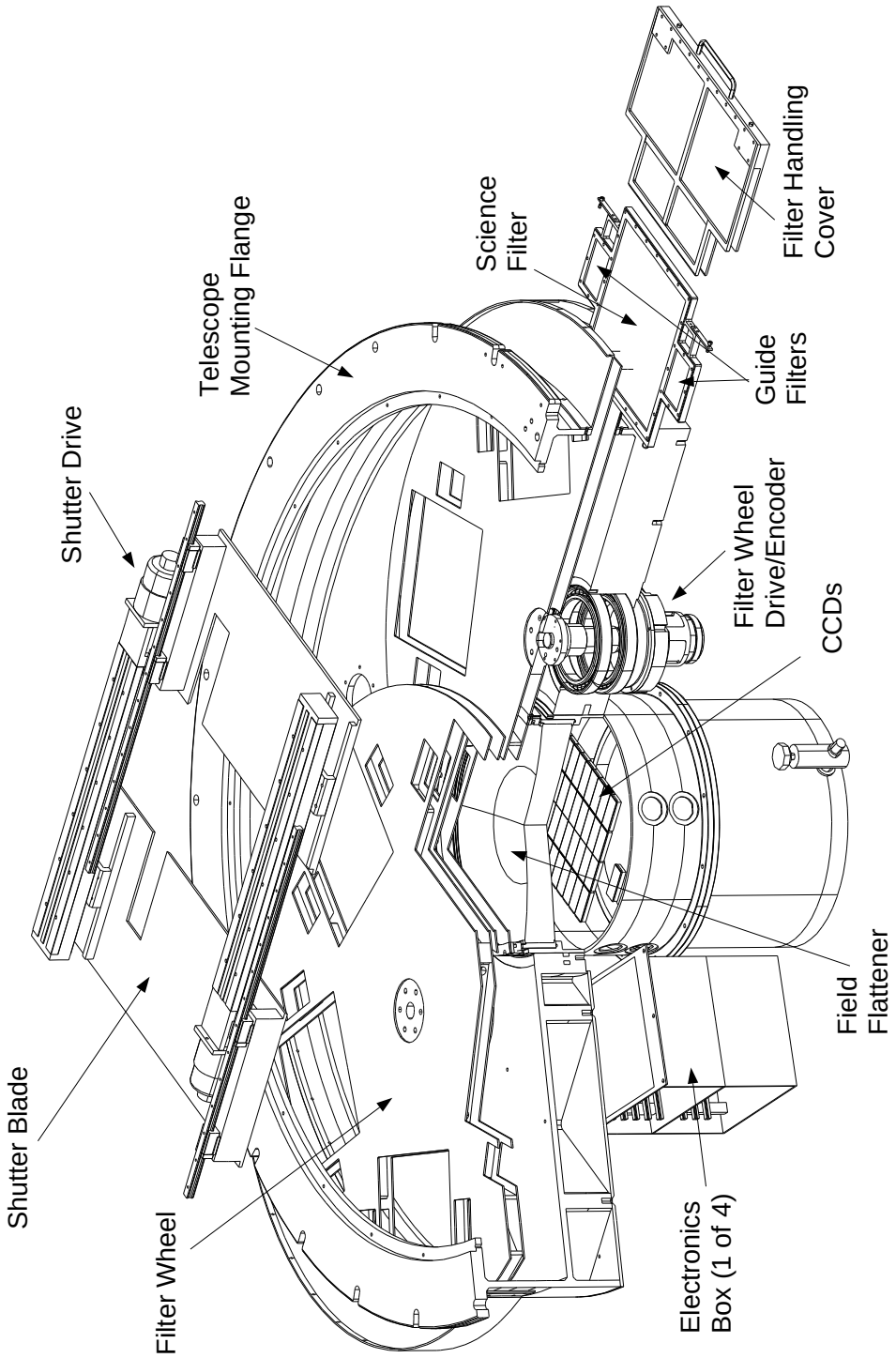

Figure 1. Cutaway and exploded view of Megacam.

2.2. Shutter

The shutter consists of two aluminum plates mounted on pairs of THK rails. Notches are cut in the shutter blades so that light reaches the guide chips when the shutter is closed. It is also possible to close the shutter completely so that no light hits the guide chips. The exposure is taken by opening one blade and ended by closing the other blade. This ensures an even exposure time over the full focal plane. A shutter blade traverses the focal plane in less than 5 sec; however, shorter exposures can be achieved by having the closing blade follow the leading blade closely, effectively scanning a slit across the focal plane. This style of shutter is used in the Big Thoughput Camera.[2] The shutter is driven from one edge with a DC servo motor and a lead-screw with a rotary encoder. The blade is attached to the other rail with a flexure to allow for differential expansion between the steel structure and the aluminum shutter blade without binding.

3. MEGACAM DEWAR

3.1. CCD Package

We have contracted with EEV Inc. to provide six CCD42-90 model thinned back-illuminated CCDs with 2048×4608 13.5μm pixels. Two of these devices will be used for evaluation in a prototype camera called Minicam. The other four will be used in the Hectospec and Hectochelle fiber spectrographs at the converted MMT.[3,4] These CCDs have a custom designed package to allow four-edge butting (see Figure 2). Signals from the silicon are wire-bonded onto a ceramic header, which wraps around to the bottom of the Invar package, where the signals are accessed from a pin grid array. A thermistor potted into the Invar is also connected to the pin grid array. Electrical connections to the CCDs are made via a modified zero-insertion-force (ZIF) socket.

The CCDs will be mounted on a 6 mm thick Invar plate, which is ground flat. This plate is thermally isolated from the Dewar case with a set of six titanium flexures mounted around the edge of the plate. The flexures allow for the 125° C temperature differential without bending the plate, which is critical for keeping all parts of the large focal plane in focus. When mounted in the mosaic, the gaps between the imaging areas will be 1 mm (corresponding to 6″) on 3 sides, and 6 mm (36″) on the fourth side.

There is no easy way to pick up four-edge buttable CCDs for installation. Thus we handle it only via a rod which screws into the back (see Figure 3). The handling rod, along with another temporary guide rod and two permanently attached locating pins, prevent the CCD from touching its neighbors as it is inserted into the focal plane. We are making no attempt to align the CCDs to each other to better than a few pixels since the camera will not be used for drift-scanning. The relative orientations will be determined by observing star clusters with known astrometry. The coplanarity of the CCDs in the mosaic is achieved by a set of precision shims attached to the Invar package by the manufacturer. These shims also provide the thermal contact between the CCD and the cold mounting plate.

3.2. Cooling

Due to the large surface area of the focal plane, the cooling of Invar CCD mounting plate must be distributed across the focal plane to avoid large temperature gradients. The cooling of the focal plane is complicated by the fact that warm preamp cards must be interspersed between the elements of the cooling transport mechanism. We are currently considering two options for cooling the CCDs to their operating temperature of −100°C, a conductive coupling, or a radiative coupling to a liquid nitrogen cryostat. The radiative coupling we are considering is similar in concept to the one used on the NOAO Mosaic camera,[5] and would consist of a set of heat fins bolted to the bottom of the cold plate. This is shown in Figure 3. A similar set of fins would be attached to the top of the LN_2 tank and would be interlaced with those on the CCD plate. Each CCD requires a total of 200-300 cm^2 fin surface area. We have successfully cooled a single dummy CCD to -100° C using this method, though no preamplifier card was present.

There are a number of advantages to radiative cooling. First, there is no mechanical coupling between the CCD mounting plate and the cryostat. This simplifies the assembly procedure. Second, the initial cooling time is reduced significantly, thus minimizing the turnaround time required for maintenance. The time required to reach within 10° C of the final temperature is expected to go from 11 h with a conductive coupling to 4 h with radiative coupling. This difference is explained by the T^4 dependence of the radiative coupling compared with the linear dependence of conductivity.

However, the radiative coupling requires high-emissivity surfaces on the fins to be efficient. We experimented with Type-I Class-2 black chromic acid anodization on a grit-blasted surface, with an estimated emissivity of 0.8,

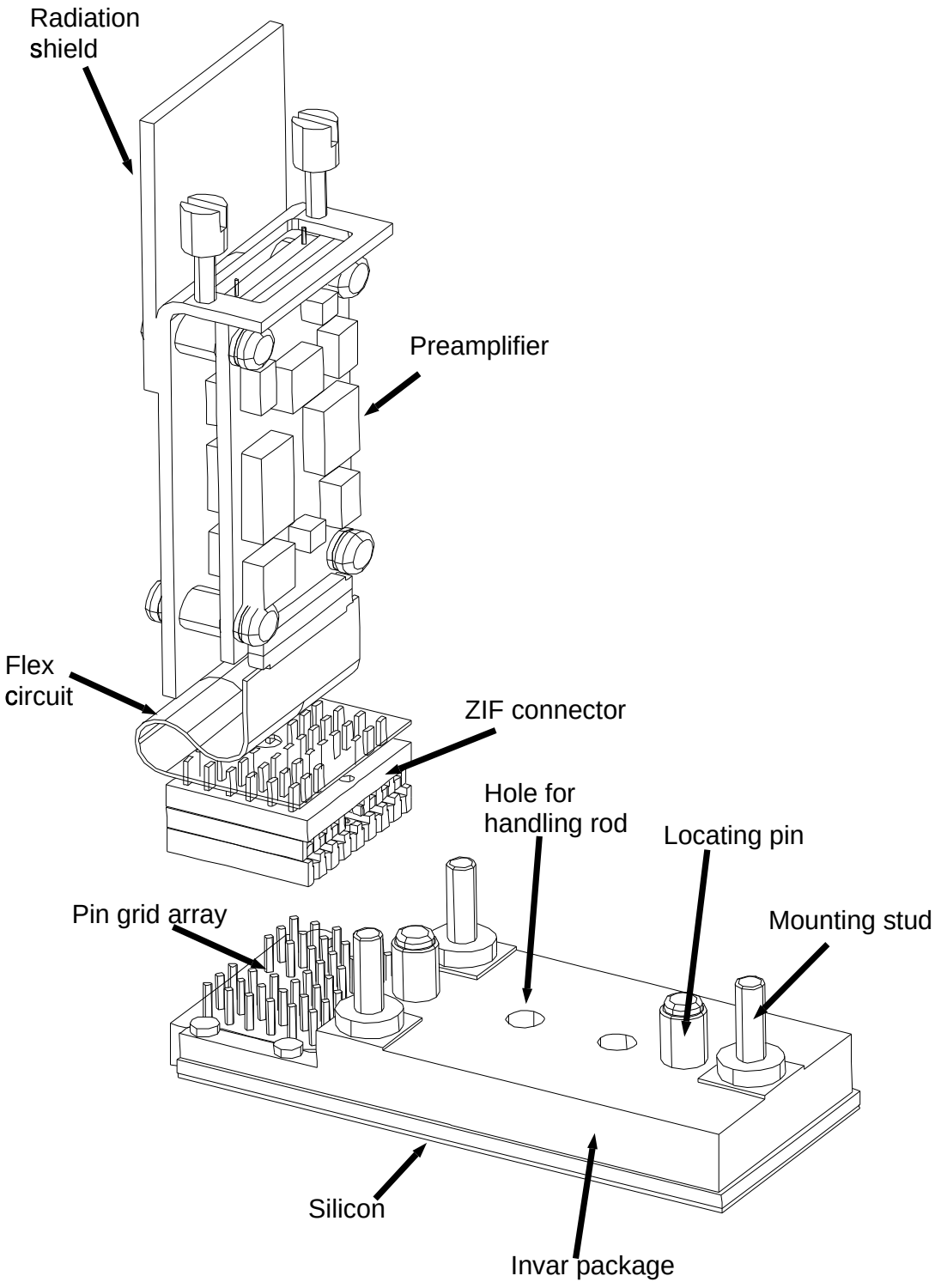

Figure 2. CCD42-90 connected to preamp card via flex circuit.

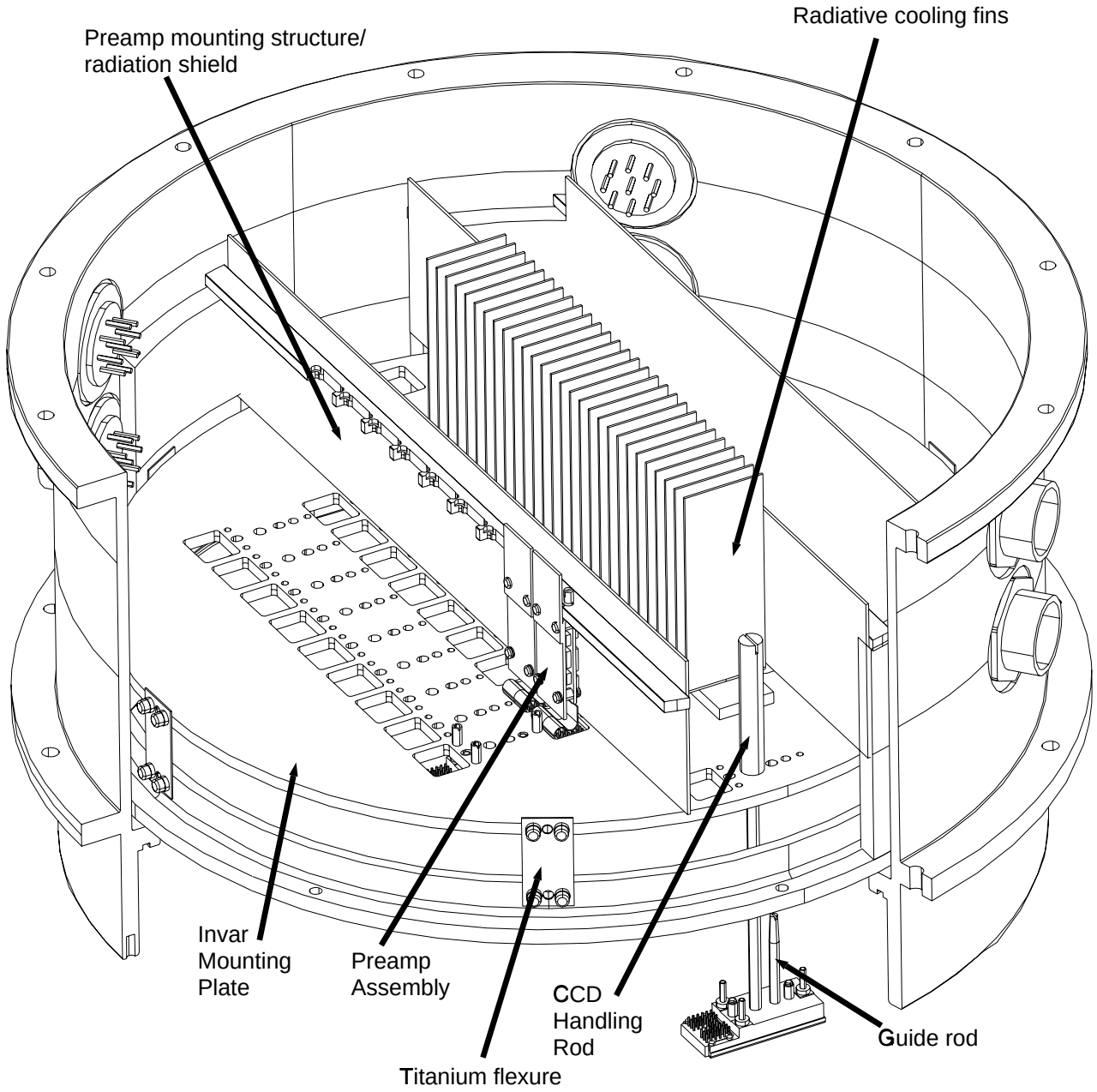

Figure 3. Underside of Megacam focal plane partially populated with CCDs. One row of CCDs is fully installed, including a set of thermal cooling fins. The row to its left shows two CCDs installed with preamp cards, and on the leftmost row, one CCD is installed without a preamp. Also shown is a guide CCD being installed. The cold Invar CCD mounting plate is suspended from the dewar case by six titanium flexures.

and the Ames-24E2 coating,[6] with emissivity 0.9. The higher emissivity of Ames-24E2 was a better radiator, but bits of this gritty coating tended to scrape off during the assembly proccess. Excellent shielding between the fins and the warm parts of the dewar, including the preamp cards, is of critical importance for keeping LN2 consumption to a minimum and, more importantly, to allow the CCDs to reach the desired temperature. We plan to experiment with both conductive and radiative methods in the Minicam dewar before making a final commitment for Megacam.

4. ELECTRONICS

Here we provide an overview of the signal chain from the CCD to the computer. Details of the electronics are described in an accompanying paper in this volume.[7]

4.1. Flex Cables

Connections between the preamplifier board and the CCD ZIF connectors will be made via a custom printed flex cable. The flex cable will serve to thermally decouple the cold CCD from the warm preamplifier. To minimize the thermal conductivity we plan to print the flex cable with Constantan traces.

4.2. Electronics

The CCD electronics will be housed in four boxes surrounding the dewar. One box will serve as the master and will generate clock signals and communicate with the host computer. Each of the four boxes will be responsible for driving signals for nine CCDs and digitizing the data from their 18 output amplifiers, before bussing the data back to the master box for transmission to the host computer. The CCDs will be clocked at 200 kilopixels s^{-1}, yielding a readout time of 24 s at full resolution, or 3 s if the pixels are binned 3×3 to $0\farcs24$.

4.3. Computer Interface

We are building a prototype set of electronics using the EDT SDV-RCI SBus card and optical fiber link. Commands to the electronics are transmitted over the fiber on a 110 Kbaud channel. With this interface we are able to achieve sustained 20 Mbyte s^{-1} transfer and disk capture to a dual processor 167 MHz Sun UltraSparc 2. This speed is more than adequate for Minicam. For Megacam we anticipate using the faster PCI-RCI version of the EDT interface to a PCI-bus based Sparcstation. This interface will be able to handle the 29 Mbyte s^{-1} rate of Megacam over a single optical fiber link. Results of data throughput tests with the prototype system are presented elsewhere in this volume.[8]

5. GUIDING WITH DEFOCUSSED IMAGES

We have chosen to incorporate the guiding directly into the focal plane using additional large format arrays. This offers several advantages over the traditional guide camera with a roving pickoff mirror: 1) with our large focal plane, and fast beam, there is no room for an unvignetted pickoff mirror above the focal plane; 2) there are no moving parts to design or worry about; and 3) because the guide detectors are firmly attached to the same focal plane as the science mosaic, they will always be confocal. We are exploiting this final feature to provide Megacam with autofocussing as well as an autoguiding capability. Guiding will be done with two guide stars, one on each CCD. Each of the two guide CCDs will have its own filter, with the thickness chosen so that one guide CCD is operated slightly inside the focus of the main mosaic, and the other slightly outside focus. If the focus drifts, one guide image will become sharper and the other will become fuzzier. Having the capability to track the focus is important on the converted MMT, because the seeing is expected to be very good, and the fast focal ratio of the primary (1.25) makes the system very sensitive to temperature changes ($2''$ of image diameter per $^\circ$ C). In addition to tracking and focus errors, we anticipate being able to detect coma to correct telescope collimation.

The aberrations will be determined by subtracting the two guide-star images from the two CCDs from each other. One of the images is rotated by 180°, and the intensities of both images are normalized before the subtraction. The difference image contains information relating to the aberrations. For example, if the telescope is out of focus, one defocussed image will be closer to focus than the other. The difference image will be negative in the center and positive away from the center (or vice versa). If there are no aberrations, the difference signal is zero. Figure 4 shows examples of the various aberrations.

To analyze the difference image, we will bin it to a 3×3 pixel image, which we treat as a 9 element vector. Through numerical simulations, we can generate corresponding basis vectors corresponding to each of the aberrations. To

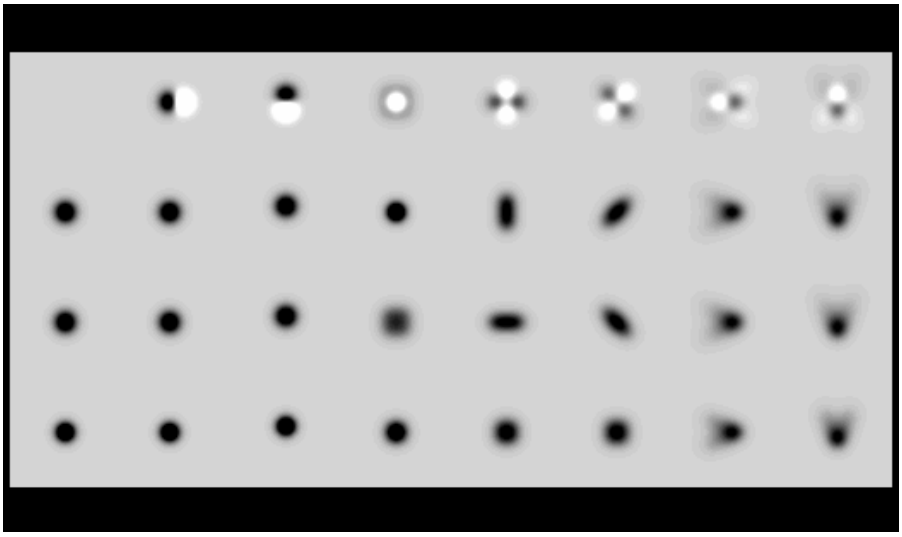

Figure 4. The rows, from bottom to top show the in-focus, inside, outside, and difference images. The columns, left to right, show the signatures of the aberrations: no aberrations, x-tilt, y-tilt, defocus, x-astigmatism, y-astigmatism, x-coma, y-coma.

determine what aberrations are present in a given observed image, we perform a linear least squares fit to find the optimal sum of the basis images that yields the observed image. This assumes that the difference image is linear with the amplitude of the aberrations, which is a reasonably good assumption for small aberrations.

5.1. Simulations

We have run a number of simulations to determine the error in the fit due to noise for a variety of conditions. Table 1 lists the resulting noise level in a single exposure with the specified number of total electrons. We assume $5e^-$ read noise per binned pixel. The amount of defocus is quoted in terms of the geometric image diameter in arcseconds. The tilt is in terms of the image motion in arcseconds. (In terms of Zernike aberrations, 1 μm of tilt = $0\farcs063$, and 1 μm of defocus = $0\farcs51$.)

At f/5.4, to get $1''$ of defocus requires changing the filter thickness by 2.3 mm, or by moving the CCD 0.92 mm.

Table 1: Random errors in focus and tilt determination

Instrument Defocus	Seeing (FWHM)	Pixel size	1-σ error for $200e^-$ image		1-σ error for $2000e^-$ image	
			Tilt	Focus	Tilt	Focus
$0\farcs26$	$0\farcs6$	$0\farcs64$	$0\farcs073$	$0\farcs40$	$0\farcs013$	$0\farcs11$
$0\farcs52$	$0\farcs6$	$0\farcs64$	$0\farcs075$	$0\farcs21$	$0\farcs014$	$0\farcs056$
$1\farcs02$	$0\farcs6$	$0\farcs64$	$0\farcs089$	$0\farcs15$	$0\farcs017$	$0\farcs036$
$2\farcs55$	$0\farcs6$	$0\farcs64$	$0\farcs60$	$0\farcs32$	$0\farcs11$	$0\farcs051$

Based on our simulations, we draw the following conclusions:

- The optimal pixel size is equal to the FWHM of the image. This can be set by changing the binning of the CCD readout.
- Determining focus requires more photons than determining tilt. Since we expect focus to vary slowly we can coadd frames for the focus determination.
- The optimal amount of defocus for determining focus error is $D \approx 1.5 \times$ FWHM. The optimal amount for determining tilt is $D = 0$. As a compromise, $D = 1.0 \times$ FWHM, or roughly $0\farcs6$ under typical seeing conditions is a reasonable choice.

In Table 2, We tabulate the noise levels for a fixed defocus of $0\farcs6$, under various seeing conditions. The pixel size is equal to the seeing FWHM in all cases.

Table 2: Errors in focus and tilt for a defocus of $0\farcs6$.

Seeing	1-σ error for $200e^-$ image		1-σ error for $2000e^-$ image	
(FWHM)	Tilt	Focus	Tilt	Focus
$0\farcs4$	$0\farcs06$	$0\farcs12$	$0\farcs01$	$0\farcs03$
$0\farcs7$	$0\farcs09$	$0\farcs24$	$0\farcs02$	$0\farcs06$
$1\farcs0$	$0\farcs12$	$0\farcs41$	$0\farcs02$	$0\farcs11$
$1\farcs3$	$0\farcs15$	$0\farcs69$	$0\farcs03$	$0\farcs18$

5.1.1. Guiding Requirements

The requirements for guiding and and focus are given as $0\farcs07$ for guiding/tracking, and $0\farcs05$ geometric image diameter for focus.[9] From Table 2 we see that the guiding specification will be met if the guidestar has about 500 counts. The limiting brightness corresponds roughly to magnitude R=20.5 for a 1 second exposure. For focussing, longer integrations will be required to meet the specification with the same brightness star. Since focus errors are expected to be slow, this is acceptable. The probability of finding a guidestar of at least R=20.5 at the Galactic pole in each of two 2048×4608 guide CCDs is $> 99.9\%$.

5.1.2. Coma and astigmatism

To determine coma and astigmatism in addition to tilt and defocus is a simple matter of fitting seven basis images instead of three. The penalty for fitting all the terms is a higher noise in the derived tilt due to cross-coupling between the coma and tilt terms. Table 3 shows the resulting noise values. The values for coma and astigmatism are given in terms of the Zernike coefficients. The collimation specification corresponds to $0.3\,\mu$m of coma, so with 10000 counts we should be able to determine the coma error. There is no formal specification for astigmatism, but the sensitivity to measuring astigmatism is slightly better than that for coma. In practice we will determine the tilt and focus from a three-term fit, and the coma and astigmatism from the full seven-term fit.

Table 3: Results of fitting seven terms

Counts	Tilt	Focus	Astigmatism	Coma
200	$0\farcs33$	$0\farcs18$	1.61μm	5.01μm
2000	$0\farcs05$	$0\farcs05$	0.25μm	0.74μm
20000	$0\farcs01$	$0\farcs02$	0.06μm	0.19μm
200000	$0\farcs00$	$0\farcs01$	0.02μm	0.06μm

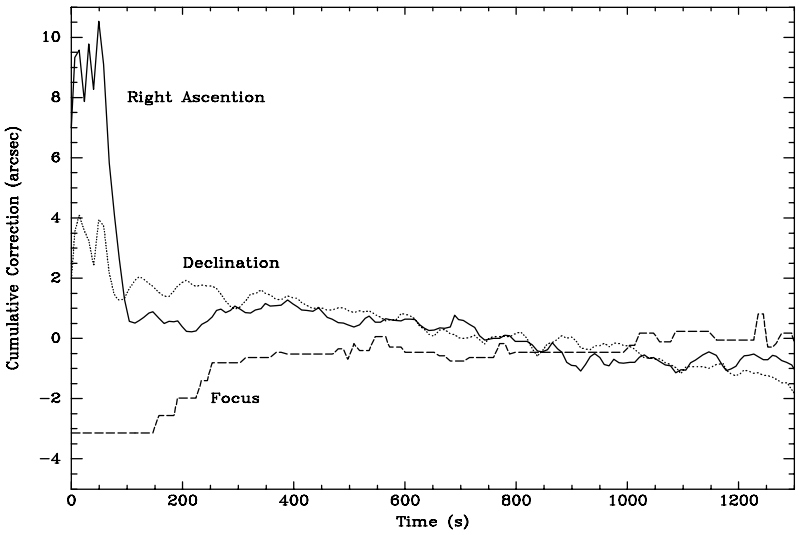

Figure 5. Commanded relative telescope pointing and focusing as a function of time while defocus-guiding was operating. The zero-point on the y-axis is arbitrary. Note that long term drifts in both tracking and focus are being corrected.

5.2. Initial Experiments

We performed an initial test of this technique to control telescope tracking and focus at the Mt. Hopkins, Arizona, 1.2 m telescope on 12 February 1998 using the 4-Shooter Camera.[10] One half of the focal plane was unfiltered, the other side had two layers of ordinary window glass (a total thickness of 4.8 mm). This causes a differential longitudinal focus of roughly 2.4 mm or a defocussed image diameter of $3''$ for each of the images. The observed seeing was $2''$-$2\farcs5$ so we had slightly more defocus than was optimal. The pixel size was $2\farcs6$, or roughly optimal. Figure 5 shows the commanded right ascension, declination, and focus as a function of time. Due to limitations in the telescope and CCD control software, we were able to take images only every 9 seconds. Initially both the focus and tracking were incorrect. The large-amplitude tracking errors were corrected first, before any focus corrections were applied. Long term drifts in both telescope tracking and focus can be seen. The gain factor for the corrections were set very low for this initial test. Unfortunately, due to poor weather we were unable to optimize the gains to achieve the most rapid correction possible. However, this initial test demonstrates that the technique can succesfully determinine tracking and focus errors simultaneously.

REFERENCES

1. B. A. McLeod, D. G. Fabricant, J. C. Geary, and A. H. Szentgyorgyi, "Wide-field CCD imager for the 6.5-m MMT telescope," in *Solid State Sensor Arrays and CCD Cameras*, C. N. Anagnostopoulos, M. M. Blouke, and M. P. Lesser, eds., *Proc. SPIE* **2654**, pp. 233–238, 1996.
2. D. Wittman, J. A. Tyson, G. M. Bernstein, D. R. Smith, R. W. Lee, M. M. Blouke, I. P. Dell'Antonio, and P. Fischer, "Big throughput camera: The first year," in *Optical Astronomical Instrumentation*, S. D'Odorico, ed., *Proc. SPIE* **3355**, pp. ?–?, 1998.
3. D. G. Fabricant, E. H. Hertz, A. H. Szentgyorgyi, R. G. Fata, J. B. Roll, and J. Zajac, "Construction of the Hectospec: a 300 optical fiber-fed spectrograph for the converted MMT," in *Optical Astronomical Instrumentation*, S. D'Odorico, ed., *Proc. SPIE* **3355**, pp. ?–?, 1998.
4. A. H. Szentgyorgyi, L. W. Hartmann, P. N. Cheimets, D. G. Fabricant, M. R. Pieri, and Y. Zhou, "Hectochelle: a multi-object echelle spectrograph for the converted MMT," in *Optical Astronomical Instrumentation*, S. D'Odorico, ed., *Proc. SPIE* **3355**, pp. ?–?, 1998.

5. T. Boroson, R. Reed, W.-Y. Wong, and M. P. Lesser, "Development of a 8192x8192 CCD mosaic imager," in *Instrumentation in Astronomy VIII*, D. L. Crawford and E. R. Craine, eds., *Proc. SPIE* **2198**, pp. 877–885, 1994.
6. S. Smith, *Formulation of Ames24E IR-Black Coating*, NASA Technical Technical Memorandum 102864, 1991.
7. J. C. Geary and S. M. Amato, "Camera electronics for the 72-channel SAO megacam," in *Optical Astronomical Instrumentation*, S. D'Odorico, ed., *Proc. SPIE* **3355**, pp. ?–?, 1998.
8. M. Conroy, J. B. Roll, W. Wyatt, D. Mink, and B. A. McLeod, "Coping with data deluge: a data system for the Megacam," in *Optical Astronomical Instrumentation*, S. D'Odorico, ed., *Proc. SPIE* **3355**, pp. ?–?, 1998.
9. D. Fabricant, B. McLeod, and S. West, *Optical Specifications for the MMT Conversion (v.6b)*, SAO, ftp://spectra.harvard.edu/pub/mmt_conv6b.ps, 1997.
10. A. Szentgyorgyi, S. Amato, D. Fabricant, R. Fata, J. Geary, C. Hughes, B. McLeod, M. Ordway, W. Wyatt, H. Epps, and M. Lesser, "Two blue-sensitive CCD cameras for the Whipple Observatory 1.2 meter telescope," *in preparation* , 1998.